Domain wall motions in BST ferroelectric thin films in the microwave frequency range

Kevin Nadaud, Caroline Borderon, Raphaël Renoud, Areski Ghalem, Aurelian Crunteanu, Laure Huitema, Frédéric Dumas-Bouchiat, Pascal Marchet, Corinne Champeaux, Hartmut W Gundel

Domain wall motions in BST ferroelectric thin films in the microwave frequency range

Kevin Nadaud,[1, 2, a)] Caroline Borderon,[3, b)] Raphaël Renoud,[3] Areski Ghalem,[2] Aurelian Crunteanu,[2] Laure Huitema,[2] Frédéric Dumas-Bouchiat,[4] Pascal Marchet,[4] Corinne Champeaux,[4] and Hartmut W. Gundel[3]

[1)] *GREMAN, UMR CNRS 7347, Université François Rabelais de Tours, 16 rue Pierre et Marie Curie, 37071 Tours Cedex 2, France*

[2)] *XLIM, UMR CNRS 7252, Université de Limoges, 123 avenue Albert Thomas, 87060 Limoges, France*

[3)] *IETR, UMR CNRS 6164, Université de Nantes, 44322 Nantes, France*

[4)] *Univ. Limoges, CNRS, SPCTS, UMR 7315, 12 rue Atlantis, F-87068 Limoges, France.*

The existence of domain wall motion at microwave frequencies and its contribution to the ferroelectric complex permittivity is shown by evaluating the dielectric properties of $BaSrTiO_3$ (BST) thin films as a function of the incident power. Even at low AC field amplitudes, the presence of the domain walls and the correlated motions (vibration and jumps) result in sensitivity of the dielectric properties to the incident field amplitude. Although the contribution of domain wall motion to the real part of the permittivity is not preponderant (less than 10 %), it represents more than 50 % of the material's global dielectric losses. This illustrates the importance to consider domain wall motion even in the microwave frequency region and the necessity to take into account the applied AC field amplitude (and thus the incident power) when characterizing ferroelectric materials. The present study has been realized on BST thin films, elaborated by pulsed laser deposition on MgO/Ir substrates.

Keywords: Ferroelectrics, domain walls, hyperbolic law, microwave frequency

[a)] Electronic mail: kevin.nadaud@univ-tours.fr

[b)] Electronic mail: caroline.borderon@univ-nantes.fr

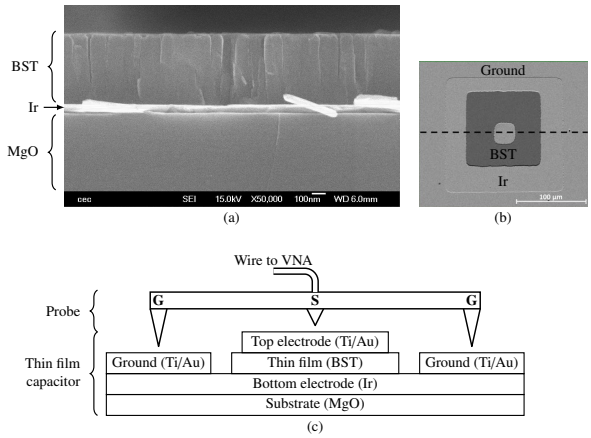

Figure 1. SEM cross section of the studied BST thin film (a), SEM top view image (b) and stack-up description (c) of the measured capacitor.

The electrically tunable permittivity of ferroelectric materials makes them interesting candidates for integration into reconfigurable microwave devices. Dielectric characterization in the microwave frequency band is mandatory in order to evaluate the frequency dependent characteristics of these materials. In the microwave range, the non-linear properties have been investigated for large AC fields[1–4] (E_{AC} large compared to E_c) but only little information is reported for low AC fields (E_{AC} small compared to E_c). In the case of ferroelectrics, even at low AC fields, non-linearity is present due to the domain wall contributions[5–8]. The permittivity depends on the measuring field amplitude E_{AC} used for the characterization according to a hyperbolic law:[7]

$$\varepsilon_r = \varepsilon_{rl} + \sqrt{\varepsilon_{r-rev}^2 + (\alpha_r E_{AC})^2}, \tag{1}$$

where ε_{rl} corresponds to the lattice contribution, ε_{r-rev} to the domain wall vibration and α_r to pinning/unpinning of the domain walls. As domain wall motion contributes to the complex permittivity, it conditions the dielectric losses and thus the figure of merit of the material[9] and consequently should not be neglected. The hyperbolic law can be applied if the AC field is sufficiently low (Rayleigh region[10]) in order to not provoke a significant change of the global polarization. Only low variation of polarization due the domain wall motions occurs[5]. The range of the validity of the hyperbolic law for the studied sample will be discussed later.

In the present paper, the existence of the domain wall motions in the microwave frequency range is shown by measuring the dielectric properties as a function of the incident power. The

study is done on an epitaxial $Ba_{2/3}Sr_{1/3}TiO_3$ thin films ((100)-oriented) elaborated by pulsed laser deposition on a (100)-oriented MgO/Ir substrate. More details on the elaboration process and the structural characterization are given elsewhere[11]. The SEM cross section micrograph of the film is shown in Fig. 1a indicating a columnar growth with grains passing through the entire film thickness. The average width of the columnar grains is about 0.1 µm for a 0.45 µm thick film. Between each grain, a boundary is present which cannot be crossed by domain walls

To begin with, the influence of the incident power on the overall dielectric properties in the microwave range is shown. The different contributions to the permittivity are then studied as a function of frequency by using the hyperbolic law. Finally, the respective weight of the different contributions to the overall permittivity and the dielectric losses is given.

The dielectric characterizations are performed in a Metal-Insulator-Metal (MIM) parallel plate capacitor geometry (Fig. 1b-1c). Following its deposition, the BST film was structured in square patterns ($100 \times 100\,\mu m^2$) using a photolithography step and wet etching. The bottom and top electrodes consist of iridium (100 nm) and gold/titanium (200 nm/10 nm), respectively, deposited by e-beam evaporation and patterned by lift-off in order to form electrodes of $30 \times 30\,\mu m^2$ surface. The measurement of the capacitor is made using a Cascade ground-signal ground (GSG) probe (125 µm pitch) and a vector network analyzer (VNA, Rohde & Schwarz ZVA24) in the 50 MHz to 2 GHz frequency range. The capacitance and $\tan\delta$ are determined using the S-parameter[12] and the permittivity is calculated using the parallel plate formula. The incident power has been varied from −20 dBm to 16 dBm. A power calibration has been performed in addition to the reflection calibration, the indicated power reported thus corresponds to the real power incident on the capacitor. The measurements have been made at room temperature (20 °C).

When using a VNA, it is necessary to convert the incident power into an incident voltage in order to obtain the electric field actually applied to the material which conditions domain wall pinning/unpinning and hence the related contribution to the permittivity. For an infinite transmission line with reference impedance Z_0 (50 Ω in our case), the magnitude of the incident voltage wave V_{AC}^+ is:

$$V_{AC}^+ = \sqrt{2 Z_0 P_{RF}}, \tag{2}$$

with P_{RF} the incident power. As the total voltage on a load corresponds to the sum of the

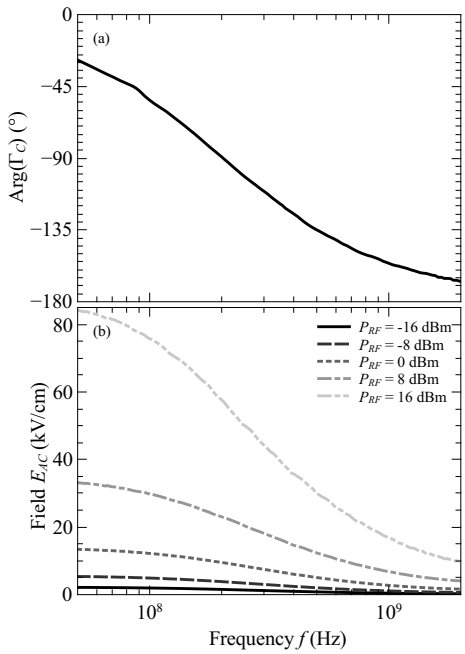

Figure 2. Phase of the reflection coefficient $\mathrm{Arg}(\Gamma_C)$ (a) and applied electric AC field E_{AC} for different incident powers (b) of the ferroelectric capacitor as a function of frequency.

incident and the reflected voltage waves, the magnitude of the voltage actually applied to the load V_{AC} is:[13]

$$V_{AC} = V_{AC}^{+} + \Gamma_C V_{AC}^{+} = |1 + \Gamma_C| \sqrt{2 Z_0 P_{RF}}, \tag{3}$$

with Γ_C the reflection coefficient of the load which can be written as:

$$\Gamma_C = \frac{1 - j\omega C Z_0}{1 + j\omega C Z_0}. \tag{4}$$

The phase of the reflection coefficient changes with increasing frequency from 0° to −180° (Fig. 2a). As a main consequence, the electric field applied to the material remains low at high frequencies (due to the prefactor $|1 + \Gamma_C|$ which tends to 0) even though the incident power increases (Fig. 2b). Depending on the capacitance value, however, the possibility to extract the different contributions to the permittivity is limited in frequency (in the present case around 1 GHz).

In order to illustrate the influence on the dielectric properties, the relative permittivity and the dielectric losses of the BST thin film as a function of frequency and for different incident powers are shown in Fig. 3. Up to 8 dBm, the permittivity and the losses increase with the incident power, which is due to the increasing contribution of domain wall pinning/unpinning. At 200 MHz, for instance, an increase of the permittivity of approximately

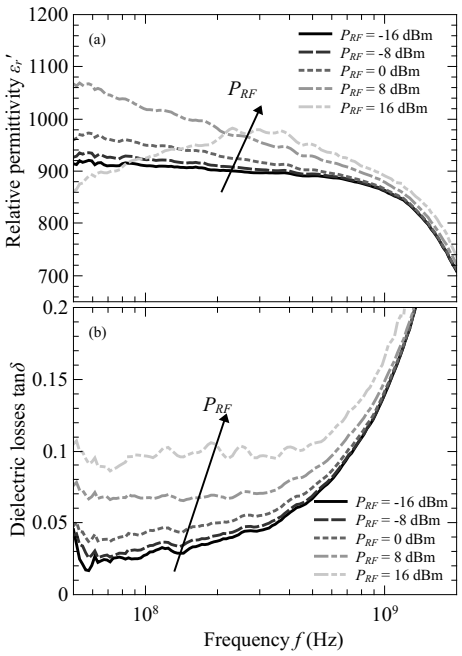

Figure 3. Relative permittivity (a) and dielectric losses (b) of the BST thin film as a function of frequency and for different incident powers.

10 % can be observed, in contrast to a 300 % huge augmentation of the losses. This confirms the very dissipative character of the domain wall pinning/unpinning contribution[6,8,9]. As the frequency increases, the influence of the incident power is less visible. This comes from the evolution of the reflection coefficient Γ_C of the capacitor which approaches -1 and results in an evolution of the AC (Fig. 2) field which is too small to cause the domain wall pinning/unpinning. The large increase of the dielectric losses with frequency and the drop of the permittivity near 1 GHz is mainly due to the losses into the electrodes which disturb the measurement[12,14,15]. Lower capacitor values would be necessary in order to determine the permittivity evolution above 1 GHz.

Finally, in the case of an incident power of 16 dBm and at low frequencies, saturation of the material is visible, which results in a lower relative permittivity and higher dielectric losses. This can be attributed to harmonic generation since a part of the incident power (at f_0) is absorbed and converted into harmonics (at kf_0)[3]. Saturation can not be seen at high frequencies since the electric field again is too small (due to the prefactor $|1+\Gamma_C|$). Heating of the material due to the incident RF power seems to be negligible as it would result in a

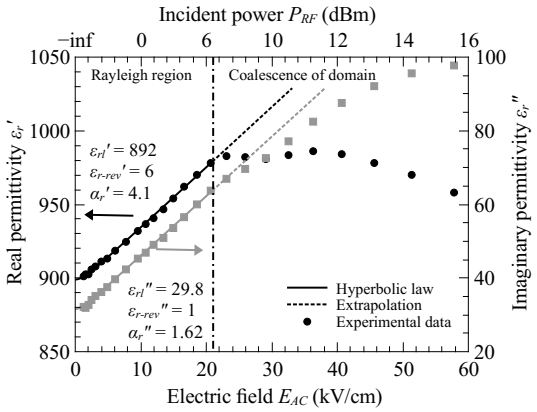

Figure 4. Real and imaginary parts of the permittivity as a function of the AC measuring field at 200 MHz and associated hyperbolic fits. The dotted curves are the extrapolation of the hyperbolic fits.

change of the permittivity in the whole frequency band, which is not the case here.

The real and the imaginary parts of the permittivity, measured as a function of the AC electric field at a frequency of 200 MHz with the associated hyperbolic fits (using the least square error method), are shown in Fig. 4. The corresponding incident power for the considered frequency is also shown. It should be noted that the E_{AC} values have to be calculated for each frequency using equation (3) since the reflection coefficient is not constant. Only the data below 20 kV/cm (Rayleigh region) are used for the hyperbolic fitting. Above 20 kV/cm the real and imaginary parts of the permittivity deviate from the hyperbolic law (dotted curves) due to the coalescence of domains and a modification of the global polarization. In this range, the AC driving field is sufficiently high for modifying the global polarization state and thus the hyperbolic law is not valid anymore. Fitting the real and imaginary parts of the permittivity allows determining the different contributions to the permittivity as a function of the frequency which are shown in Fig. 5.

The lattice contribution to the complex permittivity is shown in Fig. 5a. The real and imaginary parts have an evolution very similar to the overall material's permittivity, which is due to the fact that this is the dominant contribution. At 200 MHz, the dissipation factor of the lattice contribution ($m_l = \varepsilon_{rl}''/\varepsilon_{rl}'$) is 0.033 which is lower than the material's overall dissipation factor. While the lattice contribution represents 91 % of the real part of the permittivity, it accounts for only 46.3 % of the imaginary part (Table I). This clearly indicates that other contributions to the dielectric losses exist and have to be taken into

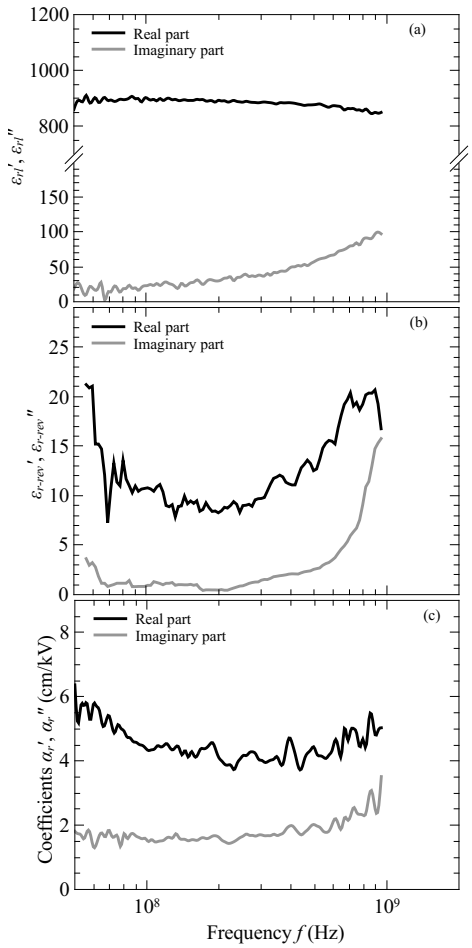

Figure 5. Real and imaginary parts of the lattice (a), vibration (b) and domain wall pinning/unpinning (c) contributions to the permittivity, as function of the frequency.

account.

The domain wall vibration contribution as a function of frequency is shown Fig. 5b. One can note that this part represents less than 1 % of the material overall permittivity. For this reason it is quite difficult to extract this contribution and the characteristic is relatively noisy. Hence, the frequency evolution of domain wall vibration can not be interpreted. According Boser[10], the domain wall vibration contribution is proportional to the domain wall density. As the value obtained here is larger than this observed for a material with spherical grains[8], the domain wall density seems to be larger. This also shows that the grain structure may influence the number of domain walls. The order of magnitude of the dissipation factor ($m_{rev} = \varepsilon''_{r-rev}/\varepsilon'_{r-rev} \approx 0.17$) is approximately 5 times larger than that of the lattice. This signifies that the domain wall vibration phenomenon is 5 times more lossy

than the lattice contribution. The main explanation for this is that more energy is needed to make vibrate a domain wall (which corresponds to change the polarization of the adjacent ferroelectric cells) than just for vibrating the lattice. As a consequence, the domain wall vibrations contribute two and a half times more into the losses (1.6 %) than into the relative permittivity (0.6 %).

The real and the imaginary parts of domain wall pinning/unpinning as a function of frequency is shown Fig 5c. The α'_r coefficient represents the sensitivity of the material to the AC electric field and thus to the incident power. In the present case, the obtained value is one order of magnitude higher compared to BST synthesized by chemical solution deposition (CSD) on alumina (about 5 instead of 0.4[8,9]). This important difference may be attributed to the particular microstructures of the materials, dense columnar in the present case (PLD on MgO/Ir single crystals) and granular in the case of CSD on ceramic alumina[8,9]. In the case of the columnar grains, domain walls can move along large distances and thus have a high contribution to the material's permittivity[10]. This high value of α'_r explains the sensitivity of the material to the AC electric field and thus to the incident power. The dissipation factor of the domain wall pinning/unpinning ($m_\alpha = \alpha''_r/\alpha'_r \approx 0.39$, at 200 MHz) is more than 10 times larger than the dissipation factor of the lattice contribution (0.033) and two times larger than this of the domain wall vibration. The domain wall pinning/unpping contribution hence is extremely dissipative which may be explain by the fact that more energy is needed to move a domain wall from one defect to another (and hence switch polarization of numerous unit cells) than for vibrating the wall. The foremost consequence is that domain wall pinning/unpinning represents 52 % of the dielectric losses but only 8.4 % of the relative permittivity. This also confirms what has been noticed before, the dielectric losses are more affected by the incident power than the relative permittivity. The weight of the different contributions to the relative permittivity and to the dielectric losses is summarized in Table I.

In conclusion, the presence and the importance of domain wall motion in the microwave region has been shown by measuring the permittivity as a function of the incident power. The study has been done on a BST thin film elaborated by pulsed laser deposition on (100)-oriented MgO/Ir substrate[11]. The different contributions to the complex ferroelectric permittivity have been analyzed with the help of the hyperbolic law[7]. Even though the weight of the domain wall contributions (vibration and pinning/unpinning) in the relative

Table I. Weight of the different contributions into the overall permittivity and dielectric losses, at frequency of 200 MHz and a electric field of 20 kV/cm (corresponding to an incident power of 6 dBm).

Contribution	Relative permittivity	Dielectric losses
Lattice	91 %	46.3 %
Domain wall vibration	0.6 %	1.6 %
Domain wall pinning/unpinning	8.4 %	52.1 %

permittivity is rather small (9 % at $E_{AC} = 20\,\mathrm{kV/cm}$), it represents almost 54 % of the dielectrics losses in the film. Domain wall motion can be qualified as very dissipative. Moreover, the presence of the domain wall pinning/unpinning phenomenon makes the material rather sensitive to the incident power (more precisely to the equivalent AC field). This has to be taken into consideration when characterizing ferroelectric materials and should be coherent with the potential application conditions. Further measurements could be done in order to determine the weight of the different contributions to the tunability by measuring the permittivity as a function of the incident power for different DC bias field as already reported for lower frequencies[9]. Additional measurements are planed to determine the frequency dispersion of the domain wall contributions by using smaller value capacitors so as to increase the frequency of the presented method.

The authors gracefully acknowledge L. Trupina and L. Nedelcu from the National Institute of Materials Physics (Romania) for the iridium bottom electrode deposition and P. Dutheil for the SEM image.

REFERENCES

[1]Y.-K. Yoon, D. Kim, M. G. Allen, J. S. Kenney, and A. T. Hunt, IEEE Transactions on Microwave Theory and Techniques **51**, 2568 (2003).

[2]J. S. Fu, X. A. Zhu, D. y. Chen, J. D. Phillips, and A. Mortazawi, in *2006 IEEE MTT-S International Microwave Symposium Digest* (2006) pp. 560–563.

[3]P. Rundqvist, A. Vorobiev, E. Kollberg, and S. Gevorgian, Journal of Applied Physics

100, 1 (2006).

[4]H. Katta, H. Kurioka, and Y. Yashima, in *2006 IEEE MTT-S International Microwave Symposium Digest* (2006) pp. 564–567.

[5]D. V. Taylor and D. Damjanovic, Journal of Applied Physics **82**, 1973 (1997).

[6]J. E. García, R. Pérez, and A. Albareda, Journal of Physics: Condensed Matter **17**, 7143 (2005).

[7]C. Borderon, R. Renoud, M. Ragheb, and H. W. Gundel, Applied Physics Letters **98**, 112903 (2011).

[8]K. Nadaud, C. Borderon, R. Renoud, and H. W. Gundel, Journal of Applied Physics **117**, 084104 (2015).

[9]K. Nadaud, C. Borderon, R. Renoud, and H. W. Gundel, Journal of Applied Physics **119**, 114101 (2016).

[10]O. Boser, Journal of Applied Physics **62**, 1344 (1987).

[11]A. Ghalem, M. Rammal, L. Huitema, A. Crunteanu, V. Madrangeas, P. Dutheil, F. Dumas-Bouchiat, P. Marchet, C. Champeaux, L. Trupina, L. Nedelcu, and M. G. Banciu, IEEE Microwave and Wireless Components Letters **26**, 504 (2016).

[12]Z. Ma, A. J. Becker, P. Polakos, H. Huggins, J. Pastalan, H. Wu, K. Watts, Y. H. Wong, and P. Mankiewich, IEEE Transactions on Electronics Devices **45**, 1811 (1998).

[13]D. M. Pozar, *Microwave Engineering, 4^{th} edition* (John Wiler & Sons, Inc., 2012) pp. 11–117.

[14]M. P. J. Tiggelman, K. Reimann, J. Liu, M. Klee, W. Keur, R. Mauczock, J. Schmitz, and R. J. E. Hueting, in *Proc. IEEE Int. Conf. Microelectronic Test Structures* (2008) pp. 190–195.

[15]A. Vorobiev, P. Rundqvist, K. Khamchane, and S. Gevorgian, Applied Physics Letters **83**, 3144 (2003).